A SIMPLE SCHEME FOR THE APPROXIMATION OF ELASTIC VIBRATIONS OF INEXTENSIBLE CURVES

SÖREN BARTELS

Abstract. A numerical scheme for the approximation of large vibration deformations of inextensible elastic curves is devised. Its unconditional stability and convergence under a mild condition on the discretization parameters are demonstrated and numerical experiments are provided.

1. Introduction

The deformation of an inextensible, incompressible, and initially straight rope, string, wire, or rod can be described by an arc-length parametrized curve $z : I \to \mathbb{R}^\ell$ with $\ell \in \{2, 3\}$ and a closed interval $I \subset \mathbb{R}$. The related elastic bending energy is given by

$$E(z) = \frac{1}{2}\int_I |z''|^2 \,\mathrm{d}x,$$

where the integrand z'' equals the curvature of the curve parametrized by z. To describe the vibrations of an evolving curve in a time interval $[0, T]$ we employ a Hamiltonian principle and consider the sum of kinetic and elastic energy given in terms of integrals on the reference configuration, i.e.,

$$H(\partial_t z, z) = \frac{1}{2}\int_I |\partial_t z|^2 \,\mathrm{d}x + \frac{1}{2}\int_I |z''|^2 \,\mathrm{d}x.$$

The evolution equations derived from this functional have to incorporate the inextensiblity constraint $|z'(t, x)|^2 = 1$ and lead to the system

$$(\partial_t^2 z, y) + (z'', y'') + (\lambda z', y') = 0, \quad |z'|^2 = 1 \text{ in } I$$

for almost every $t \in [0, T]$ and all $y \in H^2(I; \mathbb{R}^\ell)$, where λ is a scalar Lagrange multiplier associated with the pointwise constraint and $(\cdot, \cdot)$ denotes the L^2 inner product on I. The evolution equation is supplemented by initial conditions that prescribe the deformation and the velocity at $t = 0$, i.e.,

$$z(0, \cdot) = z_0, \quad \partial_t z(0, \cdot) = v_0,$$

and optional essential or periodic boundary conditions which determine the deformation or the slope at points of the boundary of I, e.g.,

$$z(\alpha, t) = z_{\mathrm{D}}(t), \quad z'(\alpha, t) = w_{\mathrm{D}}(t)$$

for $\alpha \in \partial I$. Notice that owing to the constraint $|z'(t, x)|^2 = 1$ not every choice of initial and boundary data leads to a well-posed formulation. For ease of presentation we will assume natural boundary conditions for the motivation of the numerical scheme and discuss necessary modifications for other conditions below. For the convergence analysis we need to assume that one end of the curve is fixed.

The main difficulties that arise in the numerical discretization of the hyperbolic fourth order geometric partial differential equation are the occurrence of fourth order derivatives and the nonlinear pointwise constraint. In the parabolic case of an L^2 gradient flow of the energy functional E

Date: April 2, 2014.

1991 *Mathematics Subject Classification.* 65N12, 65M60, 35L55, 53C44, 74B20.

Key words and phrases. Large vibrations, inextensible curves, elasticity, bending, finite elements.

subject to the inextensibility constraint these aspects have been addressed in [Bar13]. Therein, H^2-conforming Bézier curves have been employed and the constraint was imposed at the nodes of an underlying partition of the interval I. This allows for an efficient implementation of the proposed scheme since the derivatives of the discrete curves at the nodes are independent degrees of freedom which prescribe the tangents of the curve at the corresponding displaced nodes. It is the aim of this article to show that this approach can also be employed to simulate large vibrations of curves. Our work is inspired by analytical results in [MM03] that derive the elastic energy of inextensible curves by a rigorous dimension reduction from three-dimensional elasticity within the framework of Γ-convergence. While several results are available on the approximation of the elastic flow of curves, see, e.g., [DKS02, Poz07, DD09, BGN10, BGN12, Bar13], the author is unaware of numerical methods for the simulation of vibrating curves.
Straightforward calculations show that the evolution is entirely determined by restricting to tangential test functions, i.e., it suffices to determine a mapping $z : [0,T] \to H^2(I;\mathbb{R}^\ell)$ such that for almost every $t \in [0,T]$ we have

$$(\partial_t^2 z, y) + (z'', y'') = 0, \quad |z'|^2 = 1 \text{ in } I$$

for all $y \in H^2(I;\mathbb{R}^\ell)$ satisfying the linearized constraint

$$y' \cdot z'(t,\cdot) = 0 \text{ in } I$$

The observation that also the velocity $\partial_t z$ satisfies this condition, i.e.,

$$\partial_t z'(t,\cdot) \cdot z'(t,\cdot) = 0 \text{ in } I$$

motivates the following time stepping scheme:

$$\begin{cases} \text{Given } z^0, z^1, ..., z^k \in H^2(I;\mathbb{R}^\ell) \text{ and } v^0, v^1, ..., v^k \text{ compute } v^{k+1} \in H^2(I;\mathbb{R}^\ell) \text{ such that} \\ \quad [v^{k+1}]' \cdot [z^k]' = 0 \text{ in } I \text{ and} \\ \quad (d_t v^{k+1}, y) + ([z^k + \tau v^{k+1}]'', y'') = 0 \\ \text{for all } y \in H^2(I;\mathbb{R}^\ell) \text{ satisfying } [y]' \cdot [z^k]' = 0 \text{ in } I \text{ and set } z^{k+1} = z^k + \tau v^{k+1}. \end{cases}$$

In this scheme $\tau > 0$ is a given time step size and $d_t v^{k+1}$ denotes the backward difference quotient defined by

$$d_t v^{k+1} = \frac{1}{\tau}\big(v^{k+1} - v^k\big).$$

The operator d_t will also be applied to sequences of real numbers and we have, e.g.,

$$d_t a^{k+1} \cdot a^{k+1} = \frac{1}{2} d_t |a^{k+1}|^2 + \frac{1}{2}\tau |d_t a^{k+1}|^2$$

which follows from a binomial formula.
The existence of a unique solution v^{k+1} in every time step of the scheme is a direct consequence of the Lax-Milgram lemma and by definition of z^{k+1} we have $v^{k+1} = d_t z^{k+1}$. The iterates $(z^k)_{k=0,1,...}$ will in general not satisfy the constraint but owing to its linearized treatment and the resulting orthogonality we have

$$|[z^{k+1}]'|^2 = |[z^k]'|^2 + \tau^2 |[v^{k+1}]'|^2 = \cdots = |[z^0]'|^2 + \tau^2 \sum_{m=1}^{k+1} |[v^m]'|^2.$$

The error in the constraint is thus small provided that it is satisfied by z^0 and the sum of the spatial derivatives of the velocities v^m is bounded in an appropriate norm. This is indeed the case since a test of the discrete evolution equation with the admissible function v^{k+1} yields that

$$\frac{1}{2} d_t \|v^{k+1}\|^2 + \frac{1}{2}\tau \|d_t v^{k+1}\|^2 + \frac{1}{2} d_t \|[z^{k+1}]''\|^2 + \frac{1}{2}\tau \|[d_t z^{k+1}]''\|^2 = 0.$$

This identity proves that the total energy and in particular the velocities and certain derivatives are controlled by the initial total energy. Owing to the semi-implicit discretization some artificial numerical dissipation occurs. The resulting a priori bounds imply that the violation of the constraint is small and that the approximations admit convergent subsequences whose limits are weak solutions of the continuous problem under a non-restrictive condition on the step size. Although we restrict throughout this article to a fixed step size we remark that the arguments are also valid in the case of variable step sizes.
By replacing the function spaces in the iterative scheme by finite-dimensional subspaces and imposing the constraints at the corresponding nodes we will devise a stable and convergent numerical scheme for the computation of large vibrations of inextensible curves. The required finite element spaces and discrete time derivatives will be introduced in Section 2, the fully discrete time stepping scheme and its stability will be discussed in Section 3. A rigorous convergence analysis is presented in Section 4. In Section 5 we discuss the incorporation of a correction procedure which guarantees that the violation of the constraint remains small for large time horizons under certain conditions. The treatment of different boundary conditions such as periodic or clamped boundary conditions and the inclusion of friction terms or gravitational effects are further subjects of Section 5. Numerical experiments that illustrate the performance of the method in the case of an unwinding helix, an enforced wave, a circulating rod, vibrations of a circle, and a swinging rope are presented in Section 6.

2. Preliminaries

2.1. **Function spaces.** We let $I = [\alpha, \beta] \subset \mathbb{R}$ be a closed and non-empty interval and denote by

$$(v, w) = \int_I v \cdot w \, \mathrm{d}x$$

the L^2 inner product of scalar functions or vector fields on I with corresponding norm $\|v\|^2 = (v, v)$. Standard notation is used for Sobolev spaces, i.e., we let $H^s(I; \mathbb{R}^\ell)$ denote the set of all s-times weakly differentiable, square integrable vector fields on I with values in $\mathbb{R}^\ell$. Spatial derivatives are denoted by primes or numbers in brackets. The generalized time derivative of order j is written as $\partial_t^j v$ and we let $W^{r,p}(0, T; H^s(I; \mathbb{R}^\ell))$ for $T > 0$ denote the set of all time-dependent vector fields or families of curves w for which all generalized time derivatives up to order r define measurable mappings from $(0, T)$ with values in $H^s(I; \mathbb{R}^\ell)$ and such that the norm

$$\|v\|^p_{W^{r,p}(0,T;H^s(I;\mathbb{R}^\ell))} = \sum_{j=1}^{r} \int_0^T \|\partial_t^j v\|^p_{H^s(I;\mathbb{R}^\ell)} \, \mathrm{d}t$$

is bounded with standard modifications for the case $p = \infty$.

2.2. **Finite element spaces.** Let $\mathcal{T}_h = \{x_0 < x_1 < ... < x_M\}$ be a partition of $I = [\alpha, \beta]$ into intervals $I_i = [x_{i-1}, x_i]$ of diameter h_i, $i = 1, 2, ..., M$, and define $h = \max_{i=1,...,M} h_i$ and $h_{\min} = \min_{i=1,...,M} h_i$. Let

$$\mathcal{S}^{3,1}(\mathcal{T}_h)^\ell = \{v_h \in C^1(I; \mathbb{R}^\ell) : v_h|_{I_i} \in \mathcal{P}_3(I_i)^\ell, \, i = 1, 2, ..., M\}$$

be the space of vector fields that are piecewise cubic polynomials and continuously differentiable on I. We note that every vector field $v_h \in \mathcal{S}^{3,1}(\mathcal{T}_h)^\ell$ is determined by its nodal values $v_h(x_i)$ and $v_h'(x_i)$, $i = 0, 1, ..., M$. Given a vector field $v \in C^1(I; \mathbb{R}^\ell)$ we let $\mathcal{I}_{3,1} v$ be the uniquely determined function $\mathcal{I}_{3,1} v \in \mathcal{S}^{3,1}(\mathcal{T}_h)^\ell$ that satisfies

$$\mathcal{I}_{3,1} v(x_i) = v(x_i), \quad [\mathcal{I}_{3,1} v]'(x_i) = v'(x_i), \quad i = 0, 1, ..., M.$$

Analogously, we let $\mathcal{S}^{1,0}(\mathcal{T}_h)$ denote the space of continuous, piecewise affine functions. These are defined by their nodal values $w_h(x_i)$, $i = 0, 1, ..., M$, and we denote by $\mathcal{I}_{1,0} : C(I) \to \mathcal{S}^{1,0}(\mathcal{T}_h)$ the corresponding interpolation operator. For $w \in C(I)$ we define the discrete norms

$$\|w\|^p_{L^p_h(I)} = \int_I \mathcal{I}_{1,0}|w|^p \,\mathrm{d}x = \sum_{i=0}^{M} \beta_i |w(x_i)|^p$$

with positive numbers β_i that are the integrals of the nodal basis functions. In the case $p = 2$ we have the norm equivalence

$$\|w_h\|_{L^2(I)} \le \|w_h\|_{L^2_h(I)} \le \sqrt{3}\|w_h\|_{L^2(I)}$$

for all $w_h \in \mathcal{S}^{1,0}(\mathcal{T}_h)$. We note that for piecewise polynomial vector fields $v_h \in L^\infty(I; \mathbb{R}^\ell)$ of bounded polynomial degree we have the inverse estimates for $s \ge q$

$$\|v_h^{(s)}\|_{L^p(I_i)} \le c h_i^{q-s} \|v_h^{(q)}\|_{L^p(I_i)}$$

for $i = 1, ..., M$ and an h_i-independent constant $c > 0$. We notice the interpolation estimates for $q \ge s$ and $\mathcal{I}_h \in \{\mathcal{I}_{1,0}, \mathcal{I}_{3,1}\}$

$$\|(v - \mathcal{I}_h v)^{(s)}\|_{L^p(I_i)} \le c h_i^{q-s} \|v^{(q)}\|_{L^p(I_i)}$$

for $v \in W^{q,p}(I; \mathbb{R}^\ell)$ and with $s = 0, 1, 2, 3$ and $q \ge 2$ if $\mathcal{I}_h = \mathcal{I}_{3,1}$ or $s = 0, 1$ and $q \ge 1$ if $\mathcal{I}_h = \mathcal{I}_{1,0}$.

2.3. **Discrete time derivatives.** Given a sequence $(a^k)_{k=0,...,K}$ in a Hilbert space H and a step size $\tau > 0$ we define

$$d_t a^{k+1} = \frac{a^{k+1} - a^k}{\tau}$$

for $k = 0, 1, ..., K - 1$ and notice that

$$\langle d_t a^{k+1}, a^{k+1} \rangle_H = \frac{1}{2} d_t \|a^{k+1}\|^2_H + \frac{1}{2}\tau \|d_t a^{k+1}\|^2_H$$

We set $t_k = k\tau$ and assume that $t_K = K\tau = T$. Given any sequence of functions $(a_h^k)_{k=0,...,K} \subset L^1(I; \mathbb{R}^\ell)$ we define piecewise affine and piecewise constant interpolants $\widehat{A}, A^+, A^- : [0, T] \to L^1(I; \mathbb{R}^\ell)$ by setting for $t \in (t_k, t_{k+1})$, $k = 0, 1, ..., K - 1$,

$$\widehat{A}(t) = \frac{t - t_k}{\tau} a_h^{k+1} + \frac{t_{k+1} - t}{\tau} a_h^k, \quad A^+(t) = a_h^{k+1}, \quad A^-(t) = a_h^k.$$

We note that on every interval (t_k, t_{k+1}) we have $\partial_t \widehat{A} = d_t a_h^{k+1}$.

3. Numerical scheme

For a partition $\mathcal{T}_h = \{x_0 < x_1 < ... < x_M\}$ of $I = [\alpha, \beta]$ and a step size $\tau > 0$ such that $K\tau = T$ for some integer $K \ge 1$ our numerical scheme reads as follows.

Algorithm 1. *Let $z_h^0, v_h^0 \in \mathcal{S}^{3,1}(\mathcal{T}_h)^\ell$ and set $k = 0$.*
(1) Compute $v_h^{k+1} \in \mathcal{S}^{3,1}(\mathcal{T}_h)^\ell$ such that $[v_h^{k+1}]'(x_i) \cdot [z_h^k]'(x_i) = 0$, $i = 1, 2, ..., M$, and

$$(d_t v_h^{k+1}, y_h) + ([z_h^k + \tau v_h^{k+1}]'', y_h'') = 0$$

for all $y_h \in \mathcal{S}^{3,1}(\mathcal{T}_h)^\ell$ satisfying $[y_h]'(x_i) \cdot [z_h^k]'(x_i) = 0$, $i = 1, 2, ..., M$.
(2) Set $z_h^{k+1} = z_h^k + \tau v_h^{k+1}$.
(3) Stop if $k + 1 = K$ and otherwise increase $k \to k + 1$ and continue with (1).

The algorithm is unconditionally feasible and stable.

Proposition 3.1. *Assume that $z_h^0 \in \mathcal{S}^{3,1}(\mathcal{T}_h)^\ell$ satisfies $|[z_h^0]'(x_i)|^2 = 1$ for $i = 0, 1, ..., M$. The numerical scheme is feasible in the sense that it admits uniquely defined iterates $(z_h^k)_{k=0,...,K}$ and $(v_h^k)_{k=0,...,K}$. These satisfy*

$$\frac{1}{2}\|v_h^m\|^2 + \frac{1}{2}\|[z_h^m]''\|^2 + \frac{\tau^2}{2}\sum_{k=0}^{m-1}\left(\|d_t v_h^{k+1}\|^2 + \|[d_t z_h^{k+1}]''\|^2\right) = \frac{1}{2}\|v_h^0\|^2 + \frac{1}{2}\|[z_h^0]''\|^2 = E_{h,0}$$

for $m = 0, 1, ..., K$. Moreover, we have

$$\||[z_h^m]'|^2 - 1\|_{L_h^1(I)} \le c(\tau t_m + \tau^{1/2} t_m^{1/2}) E_{h,0}$$

for $m = 0, 1, ..., K$.

Proof. The feasibility of the numerical scheme follows from the Lax-Milgram lemma. The choice $y_h = v_h^{k+1}$ in combination with the identity $y_h^{k+1} = y_h^k + \tau v_h^{k+1}$ leads to

$$\frac{d_t}{2}\|v_h^{k+1}\|^2 + \frac{\tau}{2}\|d_t v_h^{k+1}\|^2 + \frac{d_t}{2}\|[z_h^{k+1}]''\|^2 + \frac{\tau}{2}\|[d_t z_h^{k+1}]''\|^2 = 0$$

and a summation over $k = 0, 1, ..., m-1$ prove the energy identity. The second estimate is a consequence of the relation

$$|[z_h^{k+1}]'(x_i)|^2 = |[z_h^k]'(x_i)|^2 + \tau^2 |[v_h^{k+1}]'(x_i)|^2$$

whose repeated application together with $|[z_h^0]'(x_i)|^2 = 1$ leads to

$$|[z_h^m]'(x_i)|^2 - 1 = \tau^2 \sum_{k=0}^{m-1} |[v_h^{k+1}]'(x_i)|^2.$$

A multiplication by β_i, a summation over $i = 0, 1, ..., M$, and a norm equivalence provide

$$\||[z_h^m]'|^2 - 1\|_{L_h^1(I)} \le c\tau^2 \sum_{k=0}^{m-1} \|[v_h^{k+1}]'\|^2.$$

We use the interpolation estimate $\|v'\|^2 \le c\|v\|(\|v\| + \|v''\|)$ for $v \in H^2(I; \mathbb{R}^\ell)$ to deduce that

$$\||[z_h^m]'|^2 - 1\|_{L_h^1(I)} \le c\tau^2 \sum_{k=0}^{m-1} \|v_h^{k+1}\|^2 + c\tau^{1/2}\Big(\tau \sum_{k=0}^{m-1} \|v_h^{k+1}\|^2\Big)^{1/2}\Big(\tau^2 \sum_{k=0}^{m-1} \|[v_h^{k+1}]''\|^2\Big)^{1/2}.$$

With $v_h^{k+1} = d_t z_h^{k+1}$ and the discrete energy estimates we deduce the asserted bound. □

Remark 3.1. *If the discrete velocities remain bounded in $L^2(0, T; H^1(I; \mathbb{R}^\ell))$ then we have the improved error estimate $\||[z_h^m]'|^2 - 1\|_{L_h^1(I)} \le c\tau t_m$.*

4. Convergence

Throughout this section we assume for ease of presentation that $\ell = 3$. Moreover, we consider the situation that one end of the curve is fixed or clamped, i.e., we incorporate the constraint $z_h^{k+1}(x_0) = z_{\mathrm{D}}$ or equivalently $z_h^0(x_0) = z_{\mathrm{D}}$ and $v_h^{k+1} = 0$ for all $k = 0, 1, ..., K-1$ and some $z_{\mathrm{D}} \in \mathbb{R}^3$. The stability estimates of the previous section imply that we have the inclusions

$$\widehat{V},\ V^\pm,\ \partial_t \widehat{Z} \in L^\infty(0, T; L^2(I; \mathbb{R}^3)),$$
$$Z^\pm,\ \widehat{Z} \in L^\infty(0, T; H^2(I; \mathbb{R}^3))$$

which hold boundedly as $(h,\tau)\to 0$. Notice also that we have $V^+=\partial_t\widehat{Z}$. Owing to the dissipative character of the numerical scheme we also have that the weighted sequences

$$\tau^{1/2}\partial_t\widehat{V}\in L^2(0,T;L^2(I;\mathbb{R}^3)),$$
$$\tau^{1/2}\partial_t\widehat{Z}''\in L^2(0,T;L^2(I;\mathbb{R}^3))$$

are bounded as $(h,\tau)\to 0$ in the respective spaces. The bounds allow us to select weak limits of the sequences which are compatible in the sense that, e.g., $\lim_{(h,\tau)\to 0}(V^\pm-\partial_t\widehat{Z})\to 0$, and we show that every such limit is a solution of the continuous problem in the sense of the following proposition.

Proposition 4.1. *Assume that $z\in L^\infty(0,T;H^2(I;\mathbb{R}^3))\cap H^1(0,T;L^2(I;\mathbb{R}^3))$ is such that as $(h,\tau)\to 0$ we have*

$$\widehat{Z},Z^\pm\rightharpoonup^* z\quad \text{in } L^\infty(0,T;H^2(I;\mathbb{R}^3)),$$
$$\widehat{Z}\rightharpoonup^* z\quad \text{in } W^{1,\infty}(0,T;L^2(I;\mathbb{R}^3)).$$

Assume further that $z_h^0\to z_0$ in $H^2(I;\mathbb{R}^3)$ and $v_h^0\to v_0$ in $L^2(I;\mathbb{R}^3)$ as $h\to 0$. Suppose that $\tau\le ch_{\min}^\sigma$ for some $\sigma>0$. Then z is a weak solution of the vibrating curve problem in the sense that we have $z(0)=z_0$, $|z'(t,x)|^2=1$ for almost every $(t,x)\in[0,T]\times I$, $z(t,\alpha)=z_{\rm D}$,

$$\frac{1}{2}\|\partial_t z(t)\|^2+\frac{1}{2}\|z''(t)\|^2\le\frac{1}{2}\|v_0\|^2+\frac{1}{2}\|z_0''\|^2$$

for almost every $t\in[0,T]$, and

$$\int_0^T\big\{-(\partial_t z,\partial_t y)+(z'',y'')\big\}\,\mathrm{d}t=-(v_0,y(0))$$

for every $y\in W^{1,\infty}(0,T;H^2(I;\mathbb{R}^3))$ such that $y(t,\alpha)=0$ for almost every $t\in[0,T]$ and $y'=z'\times\phi$ for some $\phi\in C^\infty(0,T;C^\infty(I;\mathbb{R}^3))$ with $\phi(T)=0$.

Proof. (1) The uniform bound for the total energy follows from a limit passage in the discrete energy identity. The attainment of the inital data follows from the identities $\widehat{Z}(0)=z_h^0$ for all $h>0$. Moreover, we deduce the boundary condition $z(t,\alpha)=z_{\rm D}$ for almost every $t\in[0,T]$.
(2) To show that the limit satisfies the constraint $|z'(t,x)|^2=1$ we notice that as a consequence of the Aubin-Lions lemma we have that $\widehat{Z}'\to z'$ pointwise almost everywhere in $[0,T]\times I$ for an appropriate subsequence and

$$\begin{aligned}\|\mathcal{I}_{1,0}|[Z^-]'|^2-1\|_{L^1(I)}=\|(\mathcal{I}_{1,0}|[Z^-]'|^2-1)^{1/2}\|_{L^2(I)}^2&\le\|(|[Z^-]'|^2-1)^{1/2}\|_{L_h^2(I)}^2\\&=\||[Z^-]'|^2-1\|_{L_h^1(I)}\le\tau^{1/2}T^{1/2}E_{h,0}\end{aligned}$$

which implies that $|[Z^-]'|\to 1$ in $L^\infty(0,T;L^1(I))$. In combination with the fact that $\|[Z^-]'-[\widehat{Z}]'\|_{L^2(I)}\le c\tau\|\partial_t\widehat{Z}'\|_{L^2(I)}$ we deduce that $|z'|=1$ almost everywhere in $[0,T]\times I$.
(3) We next discuss the limit passage in the second term of the discrete partial differential equation

$$(\partial_t\widehat{V},y_h)+([Z^+]'',y_h'')=0$$

which holds for all functions $y_h\in L^\infty(0,T;\mathcal{S}^{3,1}(\mathcal{T}_h)^3)$ with $[Z^-]'(t,x_i)\cdot y_h'(t,x_i)=0$ for $i=0,1,...,M$ and $t\in[0,T]$. Given any $\phi\in C^\infty(0,T;C^\infty(I;\mathbb{R}^3))$ with $\phi(T)=0$ that defines y as in the proposition we define an admissible discrete test function y_h by setting $y_h(t,\cdot)=\mathcal{I}_{3,1}\widetilde{y}(t,\cdot)$ for

$$\widetilde{y}(t,x)=\int_\alpha^x[Z^-]'(t,s)\times\phi(t,s)\,\mathrm{d}s$$

We then have $y_h(t,x_0)=0$ for $t\in[0,T]$ and for $i=0,1,...,M$ that

$$y_h'(t,x_i)=\widetilde{y}'(t,x_i)=[Z^-]'(t,x_i)\times\phi(t,x_i).$$

Using $\widetilde{y}''=[Z^-]''\times\phi+[Z^-]'\times\phi'$ and $[Z^+]''\cdot([Z^+]''\times\phi))=0$ we see that

$$\begin{aligned}([Z^+]'',[y_h]'')&=([Z^+]'',[\widetilde{y}]'')+([Z^+]'',[y_h-\widetilde{y}]'')\\&=([Z^+]'',[Z^--Z^+]''\times\phi)+([Z^+]'',[Z^-]'\times\phi')+([Z^+]'',[y_h-\widetilde{y}]'')\\&=-\tau([Z^+]'',[\partial_t\widehat{Z}]''\times\phi)+([Z^+]'',[Z^-]'\times\phi')+([Z^+]'',[y_h-\widetilde{y}]'')=T_1+T_2+T_3.\end{aligned}$$

After an integration in time the first term on the right-hand side satisfies

$$\begin{aligned}\int_0^T T_1\,\mathrm{d}t&\le\tau\int_0^T\|[Z^+]''\|\|[\partial_t\widehat{Z}]''\|\|\phi\|_{L^\infty(I)}\,\mathrm{d}t\\&\le\tau^{1/2}T^{1/2}\sup_{t\in(0,T)}\|[Z^+]''\|\Big(\tau\int_0^T\|[\partial_t\widehat{Z}]''\|^2\,\mathrm{d}t\Big)^{1/2}\|\phi\|_{L^\infty(0,T;L^\infty(I))}\le c\tau^{1/2}\|\phi\|_{L^\infty([0,T]\times I)}\end{aligned}$$

and hence converges to 0 as $(h,\tau)\to0$. The second term gives a contribution in the limit $(h,\tau)\to0$, i.e., owing to the Aubin-Lions lemma we have $\widehat{Z},Z^-\to z$ in $L^2(0,T;H^1(I;\mathbb{R}^3)$ and therefore

$$\int_0^T T_2\,\mathrm{d}t=\int_0^T([Z^+]'',[Z^-]'\times\phi')\,\mathrm{d}t\to\int_0^T(z'',z'\times\phi')\,\mathrm{d}t=\int_0^T(z'',y'')\,\mathrm{d}t$$

as $(h,\tau)\to0$. The third term disappears in the limit $(h,\tau)\to0$ since on every subinterval I_i we have $(Z^-|_{I_i})^{(4)}=0$ and thus, with interpolation and inverse estimates,

$$\begin{aligned}\|[y_h-\widetilde{y}]''\|_{L^2(I_i)}\le ch_i^2\|\widetilde{y}^{(4)}\|_{L^2(I_i)}&\le ch_i^2(\|[Z^-]'''\|_{L^2(I_i)}+\|[Z^-]''\|_{L^2(I_i)})\|\phi\|_{W^{3,\infty}(I_i)}\\&\le ch_i\|[Z^-]''\|_{L^2(I_i)}\|\phi\|_{W^{3,\infty}(I_i)}.\end{aligned}$$

This implies that as $(h,\tau)\to0$ we have

$$\int_0^T T_3\,\mathrm{d}t=\int_0^T([Z^+]'',[y_h-\widetilde{y}]'')\,\mathrm{d}t\to0.$$

(4) It remains to prove convergence for the kinetic term in the discrete equation. For this we note

$$y(t,x)=\int_\alpha^x z'(t,s)\times\phi(t,s)\,\mathrm{d}s=z(t,x)\times\phi(t,x)-\int_\alpha^x z(t,s)\times\phi'(t,s)\,\mathrm{d}s$$

and

$$\widehat{y}_h(t,x)=\int_\alpha^x\widehat{Z}'(t,s)\times\phi(t,s)\,\mathrm{d}s=\widehat{Z}(t,x)\times\phi(t,x)-\int_\alpha^x\widehat{Z}(t,s)\times\phi'(t,s)\,\mathrm{d}s$$

It follows that $\partial_t\widehat{y}_h\rightharpoonup\partial_t y$ in $L^2(0,T;L^2(I;\mathbb{R}^3))$ as $(h,\tau)\to0$. Moreover, we have with y_h as above

$$\|y_h-\widehat{y}_h\|_{L^2(0,T;L^2(I))}\le\|y_h-\widetilde{y}\|_{L^2(0,T;L^2(I))}+\|\widetilde{y}-\widehat{y}_h\|_{L^2(0,T;L^2(I))}\le c(h+\tau).$$

Provided that we have $\widehat{V}\to\partial_t z$ in $L^2(0,T;L^2(I;\mathbb{R}^3))$ we may thus pass to the limit in the identity

$$\int_0^T(\partial_t\widehat{V},y_h)\,\mathrm{d}t=-\int_0^T(\widehat{V},\partial_t\widehat{y}_h)\,\mathrm{d}t+(\widehat{V}(0),\widehat{y}_h(0))+\int_0^T(\partial_t\widehat{V},y_h-\widehat{y}_h)\,\mathrm{d}t$$

to deduce the missing convergence property

$$\int_0^T(\partial_t\widehat{V},y_h)\,\mathrm{d}t\to-\int_0^T(z,\partial_t y)\,\mathrm{d}t+(v_0,y(0))$$

as $(h,\tau)\to 0$. To prove the required strong convergence of $\widehat{V}$ we notice that owing to the boundedness of $(\tau^{1/2}\partial_t\widehat{V})$ in $L^2(0,T;L^2(I;\mathbb{R}^3))$ we have that

$$\int_0^{T-\delta}\|\widehat{V}(t+\delta)-\widehat{V}(t)\|_{L^2(I)}^2\,\mathrm{d}t\le c\delta$$

for all $\delta>0$ which holds uniformly as $(h,\tau)\to 0$. Moreover, we have for all $0\le t_a\le t_b\le T$ and with $V^+=\partial_t\widehat{Z}$ that

$$\overline{V}=\int_{t_a}^{t_b}\widehat{V}\,\mathrm{d}t=\int_{t_a}^{t_b}(\widehat{V}-V^+)\,\mathrm{d}t+\int_{t_a}^{t_b}\partial_t\widehat{Z}\,\mathrm{d}t=\int_{t_a}^{t_b}(\widehat{V}-V^+)\,\mathrm{d}t+\widehat{Z}(t_b)-\widehat{Z}(t_a)$$

and by an inverse estimate we have that $\overline{V}$ is uniformly bounded in $H^{\sigma/2}(I;\mathbb{R}^3)$ with $0\le\sigma\le 2$ if $\tau^{1/2}h_{\min}^{-\sigma/2}\le c$, i.e., we have, noting $\|\widehat{Z}(t)\|_{H^2(I)}\le c$ for all $t\in[0,T]$, that

$$\Big\|\int_{t_a}^{t_b}(\widehat{V}-V^+)\,\mathrm{d}t\Big\|_{H^{\sigma/2}(I)}\le(t_b-t_a)^{1/2}\Big(\tau^2\int_{t_a}^{t_b}\|\partial_t\widehat{V}\|_{H^{\sigma/2}(I)}^2\,\mathrm{d}t\Big)^{1/2}\le\tau^{1/2}(t_b-t_a)^{1/2}h_{\min}^{-\sigma/2}.$$

The compactness result of [Sim87, Thm. 1] thus implies that the sequence $(\widehat{V})_{h,\tau}$ is strongly convergent in $L^2(0,T;L^2(I;\mathbb{R}^3))$ as $(h,\tau)\to 0$. □

Remarks 4.1. *(i) The test functions y in the proposition belong for every $t\in[0,T]$ to the tangent space of $\mathcal{M}=\{\phi\in H^1(I;\mathbb{R}^3):|\phi'|^2=1\}$ at $\partial_t z(t,\cdot)$.*
(ii) Notice that the class of weak solutions specified in the proposition only satisfies an energy inequality.

5. Modifications

5.1. **Constraint correction.** The estimates of the previous section show that the proposed numerical method provides approximations that satisfy the constraint up to the error

$$\||[Z^+(t_m,\cdot)]'|^2-1\|_{L_h^1(I)}\le c\tau^{1/2}t_m^{1/2}E_{h,0}.$$

This is of practical use as long as t_m is not too large. For large time horizons it is desirable to improve the bound. A possibility is to employ a correction procedure whenever $t_m^{1/2}$ is comparable to a multiple of τ^γ for some $\gamma\in(0,1]$, i.e., to correct the approximations on a time scale which is controlled by the numerical time scale τ. The linearized treatment of the constraint implies that we have $|[z_h^m]'(x_i)|\ge 1$ for all $m=0,1,...,K$. Assuming that for some $k\ge 1$ we have

$$|[z_h^{k+1}]'(x_i)|^2-1\approx\varepsilon$$

we define $\widetilde{z}_h^{k+1}\in\mathcal{S}^{3,1}(\mathcal{T}_h)^\ell$ through the nodal values

$$\widetilde{z}_h^{k+1}(x_i)=z_h^{k+1}(x_i),\quad[\widetilde{z}_h^{k+1}]'(x_i)=\frac{[z_h^{k+1}]'(x_i)}{|[z_h^{k+1}]'(x_i)|}$$

for $i=0,1,...,M$. We then have that

$$\big|[\widetilde{z}_h^{k+1}]'(x_i)-[z_h^{k+1}]'(x_i)\big|\le\varepsilon$$

and, since the basis functions associated to derivatives scale with a factor h,

$$h^{-1}\|z_h^{k+1}-\widetilde{z}_h^{k+1}\|_{L^\infty(I)}+\|[z_h^{k+1}-\widetilde{z}_h^{k+1}]'\|_{L^\infty(I)}\le c\varepsilon.$$

If we decide to replace z_h^{k+1} by $\widetilde{z}_h^{k+1}$ we obtain the equation

$$(d_tv_h^{k+1},y_h)+([\widetilde{z}_h^{k+1}]'',y_h'')=([\widetilde{z}_h^{k+1}-z_h^{k+1}]'',y_h'')$$

where the right-hand side satisfies

$$([\widetilde{z}_h^{k+1} - z_h^{k+1}]'', y_h'') \le ch^{-1}\varepsilon \|y_h''\|_{L^2(I)}.$$

We set $\varepsilon \sim \tau^{1/2}\tau^\gamma$ which occurs after m time steps with $m \ge 0$ such that $t_m^{1/2} \sim \tau^\gamma$. The choice $y_h = v_h^{k+1}$ and a summation lead to an energy identity with the right-hand side

$$\tau \sum_{k=0}^{m-1} ([\widetilde{z}_h^{k+1} - z_h^{k+1}]'', [v_h^{k+1}]'') \le \sum_{k=0}^{m-1} \|[\widetilde{z}_h^{k+1} - z_h^{k+1}]''\|^2 + \frac{\tau^2}{4} \sum_{k=0}^{m-1} \|[v_h^{k+1}]''\|^2$$
$$\le \tau^{-2\gamma} h^{-2} \tau \tau^{2\gamma} + \frac{1}{2}\mathrm{Diss}_{h,\tau}$$

with a term $\mathrm{Diss}_{h,\tau}$ that can be absorbed. Instead of the identity $d_t z_h^{k+1} = v_h^{k+1}$ we have to employ the perturbed version

$$v_h^{k+1} = \frac{\widetilde{z}_h^{k+1} - z_h^k}{\tau} + \frac{z_h^{k+1} - \widetilde{z}_h^{k+1}}{\tau}$$

and the second term on the right-hand side related to the correction satisfies

$$\Big\| \frac{z_h^{k+1} - \widetilde{z}_h^{k+1}}{\tau} \Big\|_{L^\infty(I)} \le c\tau^{-1} h\varepsilon = ch\tau^{\gamma - 1/2}$$

which is sufficient to pass to the limit provided that $\gamma > 1/2$. Hence any choice $\gamma \in (1/2, 1]$ leads to a convergent method provided that $\tau h^{-2} \to 0$. If we have the regularity property that the term

$$\tau \sum_{k=1}^{K} \|[v_h^{k+1}]'\|^2$$

remains bounded as $(h, \tau) \to 0$, i.e., that an exact velocity satisfies $v \in L^2(0, T; H^1(I; \mathbb{R}^\ell))$, then we have $\| |[Z^+(t_m, \cdot)]'|^2 - 1 \|_{L^1_h(I)} \le c\tau t_m E_{h,0}$ and the error term in the perturbed energy law is of the order $\tau^{1+\gamma} h^{-2}$ while the error in the discrete velocities is of the order $\tau^\gamma h^{-1}$ which motivates the choice $\gamma = 1$ and leads to the condition $\tau h^{-1} \to 0$.

5.2. **Essential boundary conditions.** If the displacement of an end of the string is prescribed, i.e., an end is fixed, e.g., at $x_0 = \alpha$, we incorporate the constraint

$$v_h^{k+1}(x_0) = \partial_t z_{\mathrm{D}}(t_{k+1})$$

and impose a corresponding homogeneous version on the test functions y_h in the numerical scheme. If the end is clamped we impose the conditions

$$v_h^{k+1}(x_0) = \partial_t z_{\mathrm{D}}(t_{k+1}), \quad [v_h^{k+1}]'(x_0) = \partial_t w_{\mathrm{D}}(t_{k+1})$$

and corresponding homogeneous versions on the test functions y_h. These conditions can be combined with conditions at the end $x_M = \beta$. Periodic boundary conditions that model a closed curve lead to the constraints

$$v_h^{k+1}(x_0) = v_h^{k+1}(x_M), \quad [v_h^{k+1}]'(x_0) = [v_h^{k+1}]'(x_M)$$

and the same restrictions are imposed on the test functions y_h.

5.3. **Gravitation and friction.** A gravitational force described by a vector field $g \in L^\infty(I; \mathbb{R}^\ell)$ and frictional effects modeled by a term $-\nu\partial_t z''$ are included in the scheme by replacing the discretized partial differential equation by

$$(d_t v_h^{k+1}, y_h) + \nu([v_h^{k+1}]', y_h') + ([z_h^{k+1} + \tau v_h^{k+1}]'', y_h'') + (g, y_h) = 0.$$

If $\nu > 0$ then we obtain linear convergence of the error in the constraint, i.e., $\|\mathcal{I}_h |[Z_h]'|^2 - 1\|_{L^1_h(I)} \le c\tau\nu^{-1}$.

6. Numerical experiments

We report in this section on the practical performance of Algorithm 1 in various model situations. The constrained linear systems in every step of the algorithm were solved by introducing a Lagrange multiplier and employing a direct solver for the resulting linear systems of equations. Unless otherwise stated we always used the relation $\tau \sim h$ in the experiments. Only a few minutes were needed to compute the discrete evolutions in the examples below. In some of the experiments we employed approximate arc-length reparametrizations of given initial curves $\widetilde{z}$ obtained with the inverse of the strictly increasing function

$$\psi(r) = \int_{\widetilde{\alpha}}^{r} |\widetilde{z}'(\tau)| \, \mathrm{d}\tau,$$

i.e., the curve $z(t) = \widetilde{z} \circ \psi^{-1}(t)$ is arc-length parametrized. In our implementation we realized this by setting $z_h(x_i) = \widetilde{z}_h(\widetilde{x}_i)$ and $x_i = \psi_h(\widetilde{x}_i)$ for $i = 0, 1, ..., M$, where ψ_h is defined by numerical integration.

6.1. **Unwinding helix.** The first experiment describes the evolution of a curve that has the initial form of a partial helix without initial velocity.

Example 6.1. *Set $I = [0, 2\pi]$, $\gamma^2 = 99/100$, $\delta^2 = 1/100$, $T = 30$, and*

$$z_0(x) = \big(\sin(\gamma x), \cos(\gamma x), \delta x\big), \quad v_0(x) = 0$$

for $x \in I$. Clamped boundary conditions $z(t, 0) = (0, 1, 0)$ and $z'(t, 0) = (\gamma, 0, \delta)$ are used at $x = 0$.

Figure 1 shows snapshots of the evolution at times $t = 0$, 2, 4, ..., 28. The curvature of the initial displacement results in a velocity and the curve undergoes large deformations. In Figure 6 we plotted the discrete kinetic and elastic energies together with their sums as functions of $t \in [0, 30]$ for different discretization parameters. We observe that owing to numerical dissipation the total energy decreases while kinetic and potential energy vary.

6.2. **Enforced wave.** In our second experiment we consider a curve that is fixed at one end and periodically displaced at the other end.

Example 6.2. *Set $\widetilde{I} = [0, 4]$, $T = 15$, and let $z_0, v_0 : I \to \mathbb{R}^3$ be reparametrizations of*

$$\widetilde{z}_0(\widetilde{x}) = \Big(\widetilde{x}, \frac{4}{10}\widetilde{x}(1 - \widetilde{x}/4), 0\Big), \quad \widetilde{v}_0 = 0$$

for $\widetilde{x} \in \widetilde{I}$ such that z_0 is arc-length parametrized. Fixed boundary conditions $z(t, \alpha) = (0, \sin(t), 0)$ and $z(t, \beta) = (\beta, 0, 0)$ at both ends of $I = [\alpha, \beta]$ are used for $t \in [0, T]$.

Figure 2 shows snapshots of the evolution at times $t = 0$, 1, 2, ..., 14. We observe that a wave travels from the left end of the wire to the right end. A careful inspection of the displayed deformations for $t = 1$, 8, 15 indicates that the length of the curve changes during the evolution which is related to the violation of the pointwise constraint and the temporal growth of this error. In the left plot of Figure 7 we visualized the increase of the lengths of the discretized curves by displaying these quantities as functions of $t \in [0, 15]$ for different discretization parameters. We see that as the discretization parameters are decreased the increase of the constraint violation becomes smaller. The corresponding values of the discrete seminorms of the velocities shown in the table in Figure 7 indicate that we have the additional regularity property $v \in L^2(0, T; H^1(I; \mathbb{R}^3))$ which explains the experimental linear decay of the constraint violation error.

6.3. **Circulating rod.** A displaced rod with one clamped end and an initial velocity is specified in the following example. It leads to a circular motion of the unclamped end of the rod.

Example 6.3. *Set* $\widetilde{I} = [0,1]$, $T = 10$, *and let* $z_0, v_0 : I \to \mathbb{R}^3$ *be reparametrizations of*

$$\widetilde{z}_0(\widetilde{x}) = \big(\widetilde{x}, \widetilde{x}^2/2, 0\big), \quad \widetilde{v}_0(\widetilde{x}) = (0, \widetilde{x}, 0)$$

for $\widetilde{x} \in \widetilde{I}$ *such that* z_0 *is arc-length parametrized. A clamped boundary condition* $z(t,0) = (0,0,0)$ *and* $z'(t,0) = (1,0,0)$ *is used at* $x = 0$ *for* $t \in [0,T]$.

Figure 3 shows snapshots of the evolution at times $t = 0$, 0.2, 0.4, ..., 2.8. Since the velocity is normal to the plane spanned by the straight reference configuration and the initial deformation, a circular motion of the points on the rod takes place. Figure 8 shows the damped circular motion of the free end of the rod for two pairs of discretization parameters. We see that the numerical damping becomes smaller when the mesh and time step size are simultaneously reduced.

6.4. **Vibrations of a circle.** A periodic situation that discribes the vibrations of a circle is investigated in the fourth example.

Example 6.4. *Set* $I = [0, 2\pi]$, $T = 4$, *and let the initial parametrization* $z_0 : I \to \mathbb{R}^2$ *and the initial velocity* $v_0 : I \to \mathbb{R}^2$ *be defined by*

$$z_0(x) = \big(\cos(x), \sin(x)\big), \quad v_0(x) = 2\sin^2(x)\big(\cos(x), \sin(x)\big)$$

for $x \in I$. *Periodic boundary conditions* $z(t,0) = z(t,2\pi)$ *and* $z'(t,0) = z'(t,2\pi)$ *are imposed for* $t \in [0,T]$.

Figure 4 shows snapshots of the evolution at times $t = 0$, 0.2, 0.4, ..., 2.8. The initial velocities are outward pointing in normal direction to the circle with maxima at the north and south pole. This leads to a numerically damped periodic oscillation of the circle with symmetric displacements in north-south and east-west direction of alternating direction.

6.5. **Swinging rope.** We consider a rope that is clamped on its top end, has an initial velocity in horizontal direction, and is subject to a gravitational force in vertical direction.

Example 6.5. *Set* $I = [0,1]$, $T = 4$, *and let the initial parametrization* $z_0 : I \to \mathbb{R}^3$, *the initial velocity* $v_0 : I \to \mathbb{R}^3$, *and the gravitational force* $g : I \to \mathbb{R}^3$ *be defined by*

$$z_0(x) = \big(0, 0, -x\big), \quad v_0(x) = \big(4x^2, 0, 0\big), \quad g(x) = \big(0, 0, 40\big)$$

for $x \in I$. *The clamped boundary condition* $z(t,0) = 0$ *and* $z'(t,0) = (0,0,-1)$ *at* $x = 0$ *is imposed for* $t \in [0,T]$. *The elastic energy is scaled by the bending rigidity* $\kappa = 1/20$.

Figure 5 shows snapshots of the evolution at times $t = 0$, 0.05, 0.1, ...0.7. The rope swings within a plane and waves are travelling through the rope in longitudinal direction. Owing to the choice $\tau \sim h^2$ we do not observe significant changes in the length of the rope.

Acknowledgments. The author acknowledges the kind hospitality and support from the *Isaac Newton Institute for Mathematical Sciences* within the research programme *Free Boundary Problems and Related Topics*.

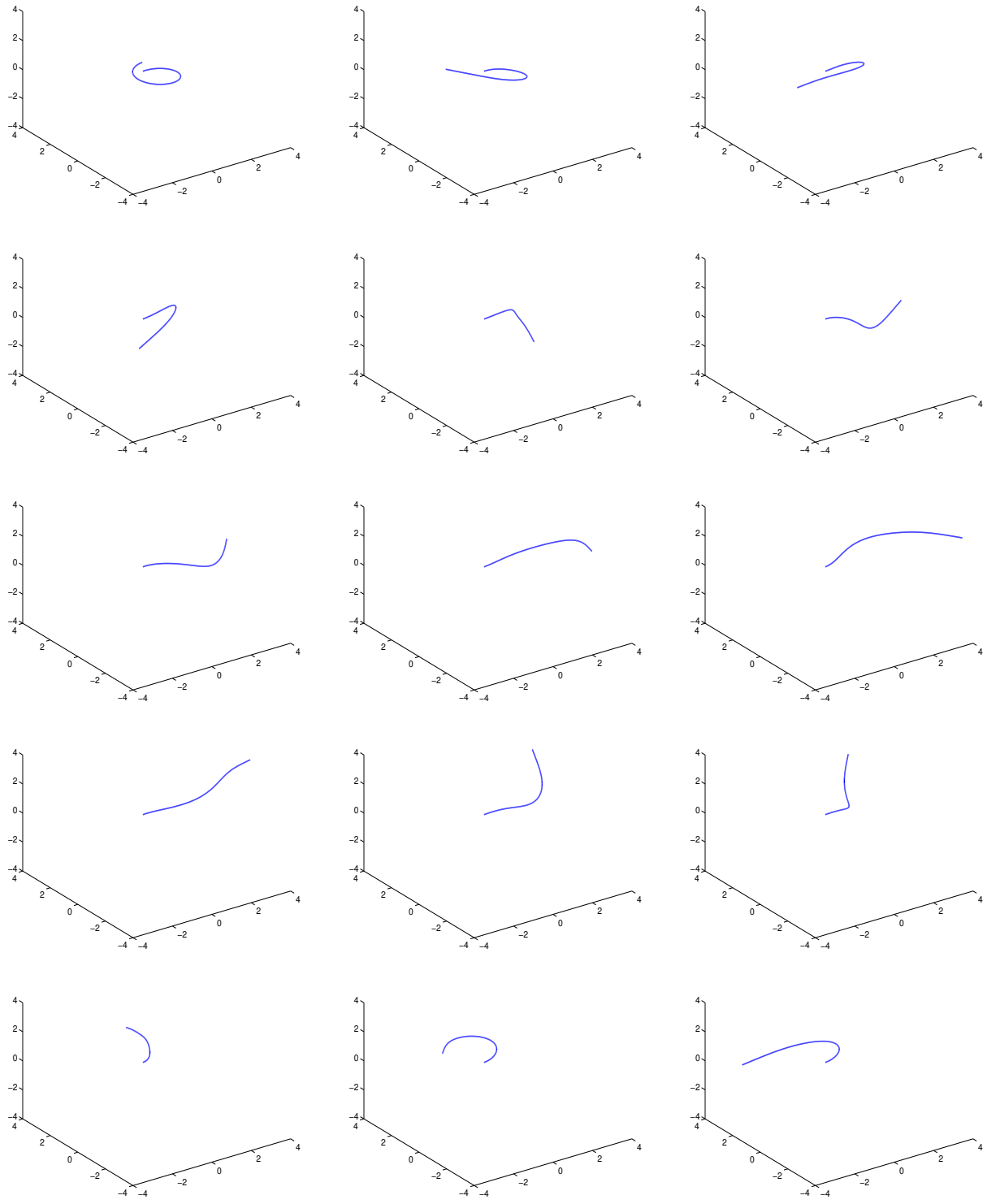

FIGURE 1. Discrete deformations $\widehat{Z}(t,\cdot)$ of a clamped helix for $t = 0,\ 2,\ ...,\ 28$ (from left to right and top to bottom) with a partition of the parameter domain $I = [0, 2\pi]$ into 40 subintervals and $\tau = 1/40$ in Example 6.1.

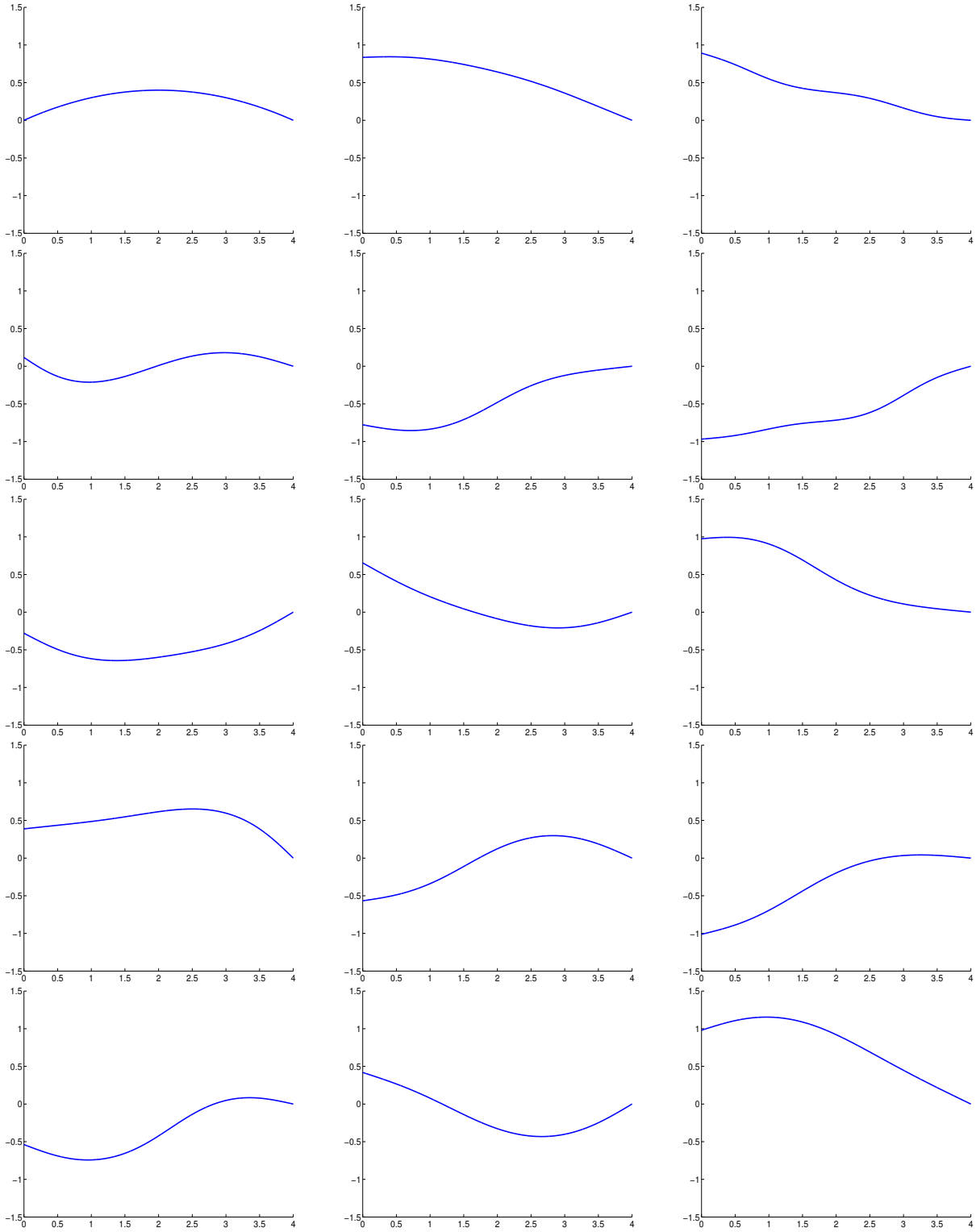

FIGURE 2. Discrete deformations $\widehat{Z}(t,\cdot)$ of a periodically displaced wire for $t = 0$, 1, ..., 14 (from left to right and top to bottom) and a partition of the parameter domain $I = [0, 4]$ into 40 subintervals and $\tau = 1/40$ in Example 6.2.

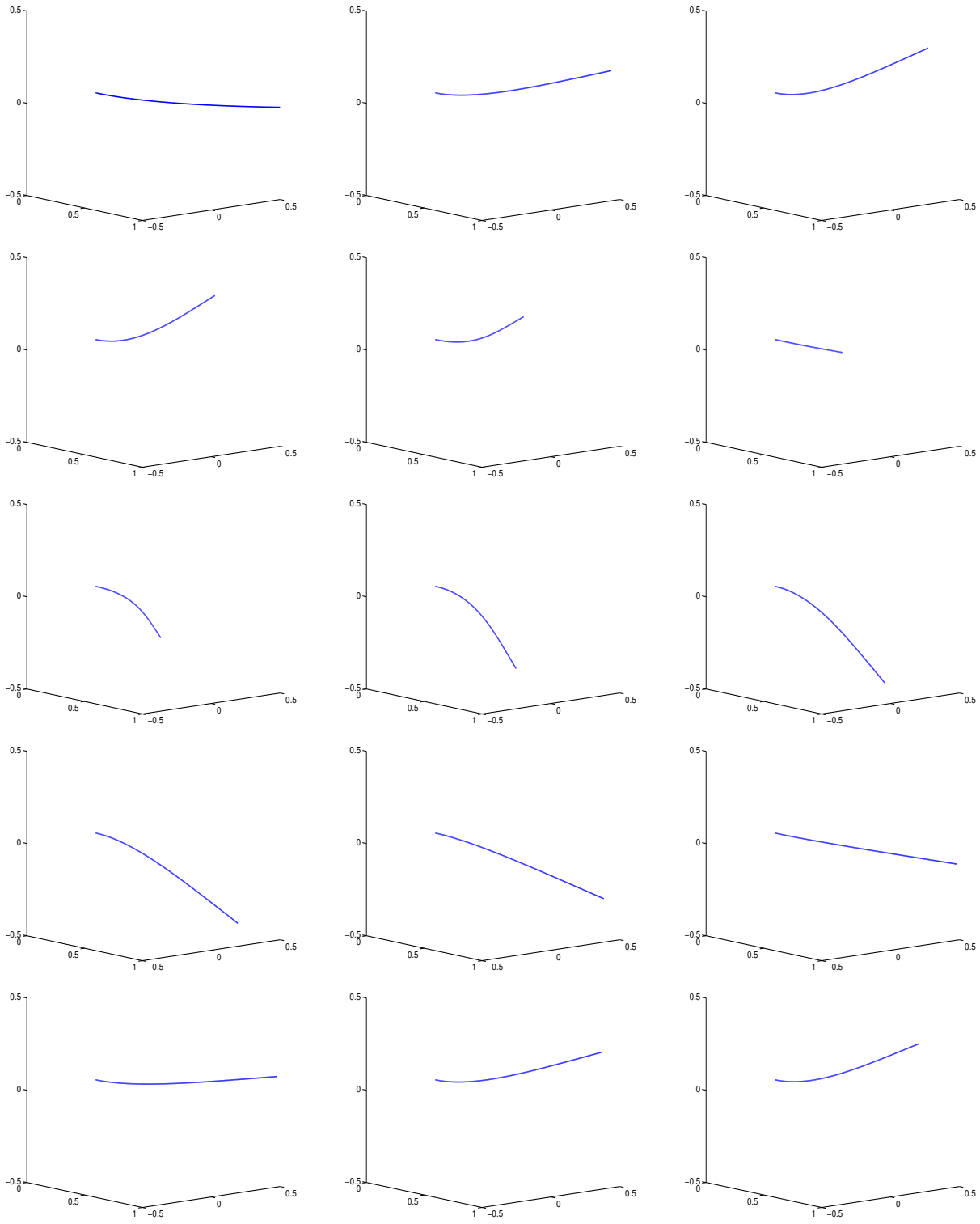

FIGURE 3. Discrete deformations $\widehat{Z}(t,\cdot)$ of a circulating rod that is clamped at one end for $t = 0$, 0.2, ..., 2.8 (from left to right and top to bottom) and a partition of the parameter domain $I = [0, 2]$ into 40 subintervals and $\tau = 1/40$ in Example 6.3.

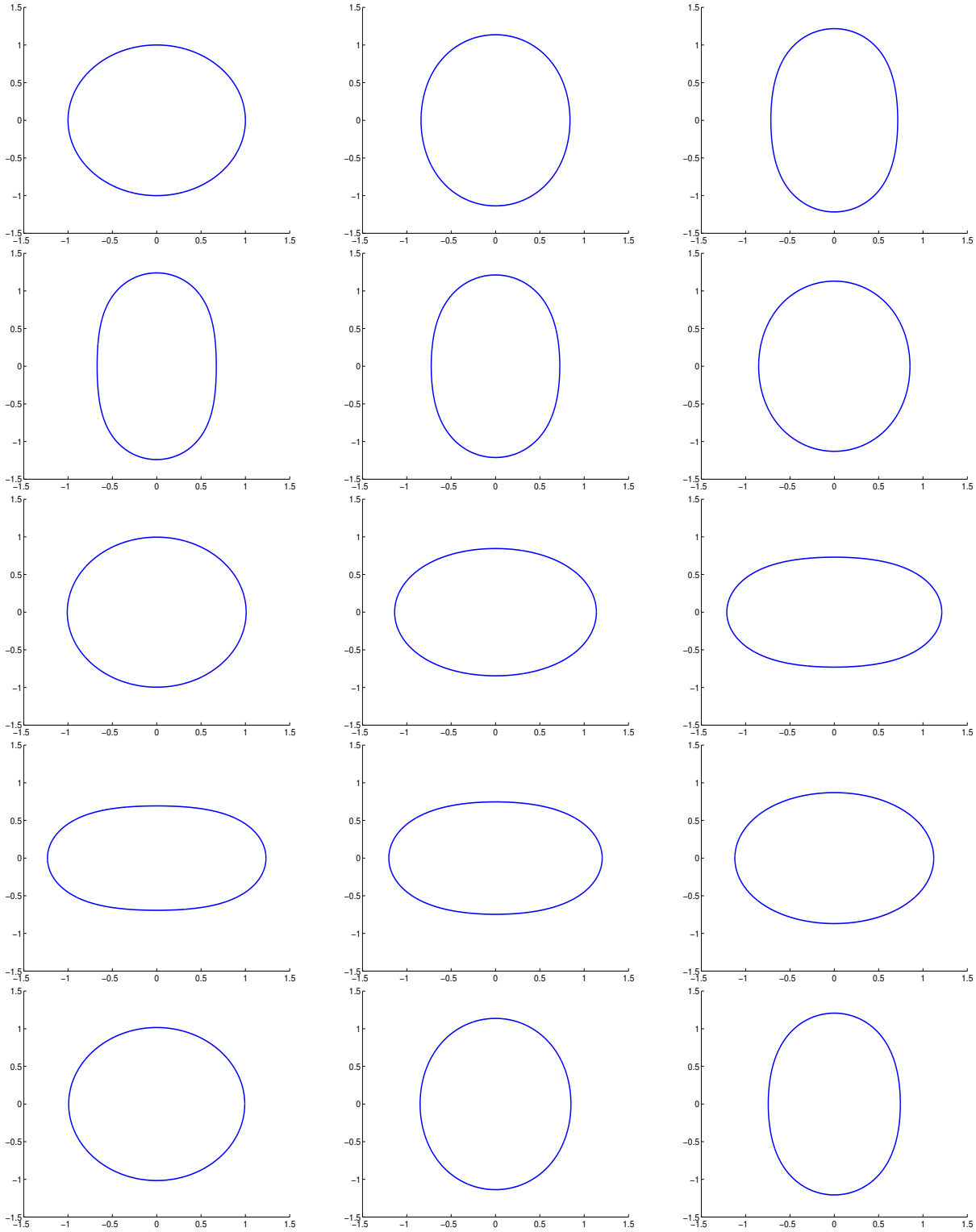

FIGURE 4. Discrete deformations $\widehat{Z}(t,\cdot)$ of a circle with normal initial velocity for $t = 0,\ 0.2,\ \ldots.\ 2.8$ (from left to right and top to bottom) and a partition of the parameter domain $I = [0, 2\pi]$ into 100 subintervals and $\tau = 1/100$ in Example 6.4.

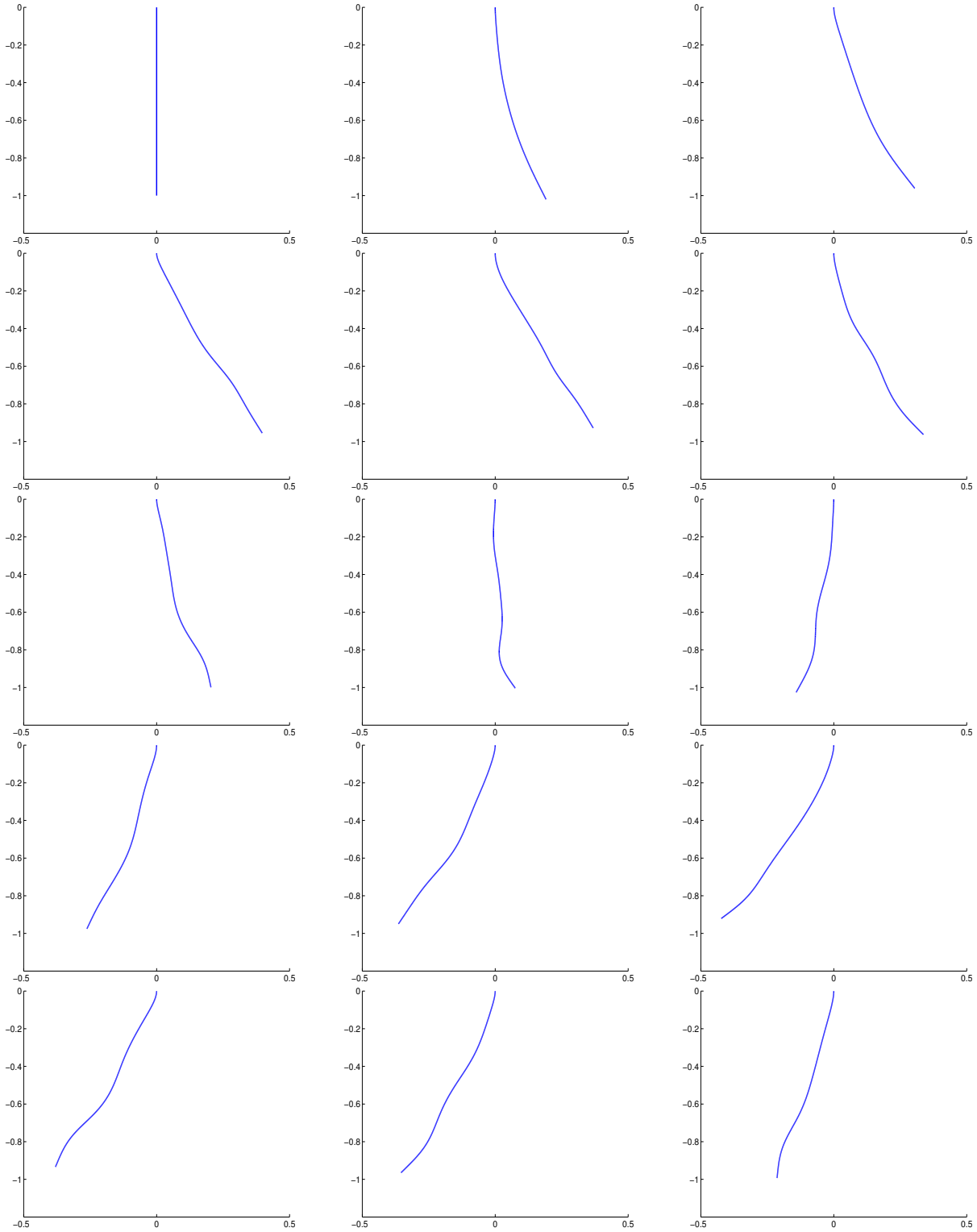

FIGURE 5. Discrete deformations $\widehat{Z}(t,\cdot)$ of a swinging rope subject to gravity with initial velocity for $t = 0$, 0.05, 0.1, ..., 0.7 (from left to right and top to bottom) and a partition of the parameter domain $I = [0,1]$ into 40 subintervals and $\tau = 1/40^2$ in Example 6.5.

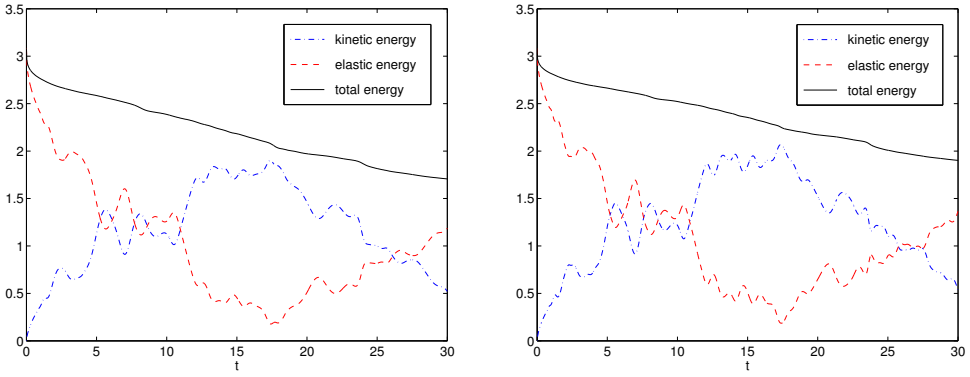

FIGURE 6. Kinetic, elastic, and total energies as functions of $t \in [0,T]$ for the discretization parameters $\tau \sim h = 1/40$ (left) and $\tau \sim h = 1/80$ (right) in Example 6.1.

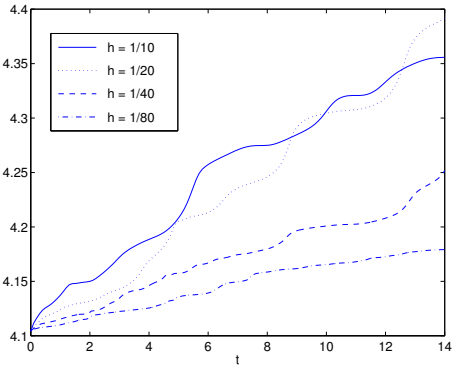

$\tau \sim h$	$\|[V^+]'\|_{L^2([0,T]\times I)}$
1/5	2.8326
1/10	2.2849
1/20	3.4676
1/40	3.4713
1/80	3.4812
1/160	5.0713
1/320	4.7537

FIGURE 7. Increase of the lengths of curves shown as functions of $t \in [0,T]$ (left) and empirical boundedness of semi-norms $\|[V^+]'\|_{L^2([0,T]\times I)}$ (right) for the discretization parameters $\tau \sim h$ and different mesh-sizes in Example 6.2.

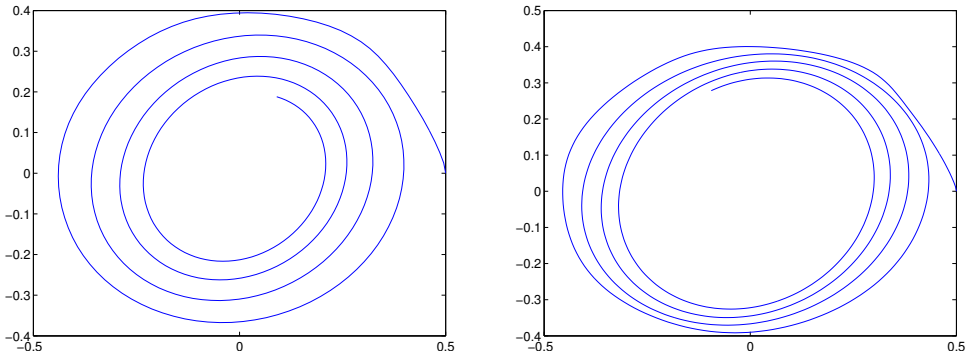

FIGURE 8. Discrete damped circular motion of the free end of the vibrating rod given by the function $t \mapsto z_h(t,1)$ for the discretization parameters $\tau \sim h = 1/40$ (left) and $\tau \sim h = 1/80$ (right) in Example 6.3.

References

[Bar13] Sören Bartels, *A simple scheme for the approximation of the elastic flow of inextensible curves*, IMA J. Numer. Anal. **33** (2013), no. 4, 1115–1125.

[BGN10] John W. Barrett, Harald Garcke, and Robert Nürnberg, *Numerical approximation of gradient flows for closed curves in* $\mathbb{R}^d$, IMA J. Numer. Anal. **30** (2010), no. 1, 4–60.

[BGN12] ———, *Parametric approximation of isotropic and anisotropic elastic flow for closed and open curves*, Numerische Mathematik **120** (2012), 489–542, 10.1007/s00211-011-0416-x.

[DD09] Klaus Deckelnick and Gerhard Dziuk, *Error analysis for the elastic flow of parametrized curves*, Math. Comp. **78** (2009), no. 266, 645–671.

[DKS02] Gerhard Dziuk, Ernst Kuwert, and Reiner Schätzle, *Evolution of elastic curves in* $\mathbb{R}^n$*: existence and computation*, SIAM J. Math. Anal. **33** (2002), no. 5, 1228–1245.

[MM03] Maria Giovanna Mora and Stefan Müller, *Derivation of the nonlinear bending-torsion theory for inextensible rods by* Γ*-convergence*, Calc. Var. Partial Differential Equations **18** (2003), no. 3, 287–305.

[Poz07] Paola Pozzi, *Anisotropic curve shortening flow in higher codimension*, Math. Methods Appl. Sci. **30** (2007), no. 11, 1243–1281.

[Sim87] Jacques Simon, *Compact sets in the space* $L^p(0,T;B)$, Ann. Mat. Pura Appl. (4) **146** (1987), 65–96.

Abteilung für Angewandte Mathematik, Albert-Ludwigs-Universität Freiburg, Hermann-Herder Str. 10, 79104 Freiburg i.Br., Germany

E-mail address: bartels@mathematik.uni-freiburg.de